SEMIACTIVE CONTROL ALGORITHMS FOR STRUCTURES WITH VARIABLE DAMPERS

By Fahim Sadek[1] and Bijan Mohraz,[2] Fellow, ASCE

ABSTRACT: Semiactive control systems combine the features of active and passive control to reduce the response of structures to various dynamic loadings. They include: (1) Active variable stiffness, where the stiffness of the structure is adjusted to establish a nonresonant condition between the structure and excitation; and (2) active variable damper, where the damping coefficient of the device is varied to achieve the most reduction in the response. This study is concerned with examining the effectiveness of variable dampers for seismic applications. Three algorithms for selecting the damping coefficient of variable dampers are presented and compared. They include a linear quadratic regulator algorithm; a generalized linear quadratic regulator algorithm with a penalty imposed on the acceleration response; and a displacement-acceleration domain algorithm, where the damping coefficient is selected by examining the response on the displacement-acceleration plane and assigning different damping coefficients accordingly. Two-single-degree-of-freedom structures subjected to 20 ground excitations are analyzed using the three algorithms. The analyses indicate that, unlike passive dampers (where for flexible structures, an increase in damping coefficient decreases displacement but increases the acceleration response), variable dampers can be effective in reducing both the displacement and acceleration responses. The algorithms are used to compute the seismic response of two structures: (1) An isolated bridge modeled as a single-degree-of-freedom system; and (2) a base-isolated six-story frame modeled as a multi-degree-of-freedom system. The results indicate that variable dampers significantly reduce the displacement and acceleration responses.

INTRODUCTION

New concepts for active and passive control have been developed for reducing the response of structures to wind, earthquake, blast, and other dynamic loadings. Passive control refers to systems that utilize the response of structures to develop the control forces without requiring an external power source for their operation. Active control, on the other hand, refers to systems that require a large power source to operate the actuators that supply the control forces, whose magnitudes are determined using feedback from sensors that measure the excitation and/or the response of the structure. Semiactive control combines the features of active and passive systems. These systems require a small power source (e.g., a battery) to operate and utilize the response of the structure to develop the control forces that are regulated by algorithms using the measured excitation and/or response.

Semiactive control systems include two categories: (1) Active variable stiffness; and (2) active variable damper. In the first category, the stiffness of the structure is adjusted to establish a nonresonant condition between the structure and excitation. Variable stiffness devices can be regulated to include or exclude the stiffness of a particular section of the structure, such as the bracing system. In the second category, supplemental energy dissipation devices, such as fluid, friction, and electrorheological dampers, are modified to allow adjustments in their mechanical properties to achieve significant reductions in the response. In both categories, like passive systems, control forces are generated using the motion of the structure and, like active systems, controllers are used to monitor feedbacks and develop the appropriate command signals for selecting the stiffness or the damping coefficient of the device.

This study focuses on the use of semiactive control algorithms for structures with variable damping devices. Several investigators have studied the suitability of variable dampers and have found them to be effective in reducing the response of structures to different dynamic loadings. In addition to requiring a small power source to operate, the control forces developed by these devices always oppose the direction of motion, thereby, enhancing the overall stability of the structure.

The next section presents a brief summary of previous work on development of semiactive control algorithms for variable damping devices. Three algorithms are then discussed, and their effectiveness in reducing the displacement and acceleration responses of structures to seismic loading is examined. The algorithms are used in several structures modeled as single-degree-of-freedom (SDOF) and multi-degree-of-freedom (MDOF) systems subjected to different earthquake excitations to demonstrate their effectiveness in reducing the response.

SUMMARY OF PREVIOUS WORK

For active variable dampers, the damping coefficient $c(t)$ during the response can be adjusted between upper and lower limits, c_{max} and c_{min}; i.e.

$$c_{min} \leq c(t) \leq c_{max} \qquad (1)$$

Several investigators have developed algorithms to select the appropriate damping coefficient during the response. Patten et al. (1993) and Sack et al. (1994) introduced a hydraulic actuator with an adjustable orifice and used a closed-loop control algorithm to select the damping coefficient of the device at each increment of time. Patten et al. and Sack et al. used a clipped optimal control algorithm based on the linear quadratic regulator (LQR) with a check on the dissipation characteristics of the control force. The results of these investigators indicate that a variable damper can significantly reduce the response of a structure to seismic forces. In another study, Patten et al. (1994a) used a bang-bang (also referred to as two-stage, bistate, or on-off) algorithm based on Lyapunov's method to select the damping coefficient. Patten et al. used the algorithm in the analysis of a three-story frame subjected to the 1979 El

[1]Res. Assoc., Southern Methodist Univ., Dallas, TX 75275; on Assignment, National Institute of Standards and Technology, Gaithersburg, MD 20899.

[2]Prof. of Mech. Engrg., Southern Methodist Univ., Dallas, TX 75275; on Leave, National Institute of Standards and Technology, Gaithersburg, MD 20899.

Note. Associate Editor: Dimitrios Karamanlidis. Discussion open until February 1, 1999. To extend the closing date one month, a written request must be filed with the ASCE Manager of Journals. The manuscript for this paper was submitted for review and possible publication on October 3, 1997. This paper is part of the *Journal of Engineering Mechanics*, Vol. 124, No. 9, September, 1998. ©ASCE, ISSN 0733-9399/98/0009-0981–0990/$8.00 + $.50 per page. Paper No. 16762.

Centro accelerogram. The variable damper reduced the response of the frame by ~54% as compared to the response with no control. Other studies have been carried out to investigate the effectiveness of similar devices in reducing the response of bridges to vehicle-induced vibrations (Patten et al. 1994b, 1996).

Feng and Shinozuka (1990, 1993) have shown that, for seismically isolated bridges, increasing the damping of the isolation system reduces the relative displacement but increases the absolute acceleration. Feng and Shinozuka suggested that the isolation system should contain a variable damper and used two algorithms for regulating the damping coefficient of the damper. One is a bang-bang algorithm where $c(t)$ is set to c_{max} when the relative displacement response divided by a referenced displacement is greater than the absolute acceleration response divided by a referenced acceleration. For the opposite case, $c(t)$ is set to c_{min}. The other algorithm is an instantaneous optimal algorithm introduced by Yang et al. (1987). Numerical results indicate reductions of ~41% in peak displacement and 22% in peak acceleration responses for the case where the bridge was subjected to the S00E component of El Centro, 1940. Kawashima and Unjoh (1993) and Kawashima et al. (1994) used a displacement-dependent damping model to select the damping coefficient of a variable fluid damper. Analytical results and shake table tests of a 30-m-long bridge indicated reductions of 24 and 44% in displacement and acceleration responses, respectively. In a later study, Yang et al. (1994) used the sliding mode control theory to design an algorithm for the variable damper suggested by Kawashima and Unjoh (1993) and Kawashima et al. (1994). The idea behind the sliding mode control theory is to drive and maintain the response trajectory into a sliding surface, where the motion of the structure is stable. Numerical results indicate that further reductions in the seismic response of the bridge can be achieved using the sliding mode algorithm.

Dowdell and Cherry (1994a,b) used a bang-bang semiactive LQR algorithm to control the slip forces in friction dampers. Dowdell and Cherry computed the responses of an SDOF structure and a six-degree-of-freedom structure to a band-limited white noise excitation with and without semiactive friction dampers. The results indicated significant reductions in the interstory drifts of the structures. In another study, Yang and Lu (1994) introduced a multistage semiactive friction damper to reduce the seismic response of cable-stayed bridges and demonstrated numerically the effectiveness of the damper. Loh and Ma (1994) used a bang-bang semiactive algorithm based on Lyapunov's theory for a three-story frame and showed that the effect of variable dampers on the response can be significant. Calise and Sweriduk (1994) used robust control techniques for variable damping devices and demonstrated their effectiveness in reducing the response.

In an extensive analytical and experimental study, Symans and Constantinou (1995) developed and tested a two-stage damper and a variable semiactive fluid damper. For the two-stage damper, a base shear coefficient and a force transfer control algorithm were used, while for the variable damper, a feedforward, a skyhook damping, an LQR, and a sliding mode control algorithm were employed. Symans and Constantinou's study included a single-story frame and a three-story frame under different seismic excitations. The results indicated that while variable dampers significantly reduced the response as compared to the case with no control, no reduction was observed when compared to the device acting as a passive damper with a damping coefficient c_{max}.

The study by Symans and Constantinou (1995) indicates that the use of semiactive dampers in structures is inefficient when compared to passive systems. Since Symans and Constantinou's study was limited to an SDOF structure with a period of 0.36 s and an MDOF structure with a fundamental period of 0.56 s, the efficiency of the device for other periods merits further investigation. This study considers a broad range of periods for which semiactive control with variable dampers may be more efficient than passive dampers in reducing the response. In the following sections, three semiactive control algorithms are examined to determine the effectiveness of variable dampers in reducing the seismic response. A semiactive variable device with a damping coefficient between c_{min} and c_{max} and the same device acting as a passive damper with damping coefficients c_{min} and c_{max} are compared to assess the effectiveness of the variable damper.

ANALYSIS

Increased damping in structures allows the dissipation of a larger portion of the input energy and, consequently, a further reduction in the response. The reduction, however, depends on the flexibility or rigidity of the structure. Feng and Shinozuka (1990, 1993) have reported that for isolated bridges, increased damping has opposite effects on the absolute acceleration of the girder and the relative displacement between the girder and the piers. A similar observation was made by Sadek et al. (1996), who showed that for flexible structures (defined in this study as structures with periods equal to or longer than 1.5 s) an increase in damping further decreases the displacement response and usually increases the acceleration response and consequently the seismic forces. Variable dampers, where the damping coefficient can be adjusted between an upper and a lower limit, may be effective in reducing both the relative displacement and absolute acceleration responses. Reducing the absolute acceleration response is important in the design of structures, such as hospitals, communication centers, computer and electronic facilities, etc., which house sensitive equipment that may be damaged by large floor accelerations. In addition, in retrofit of existing structures, the use of passive dampers may increase accelerations and consequently, seismic forces and story shears where the increase may not be permitted by the capacity of the existing lateral force resisting system. Large accelerations may also cause discomfort to occupants.

To illustrate the influence of supplemental damping and structural period on the seismic response of structures, six-SDOF structures with periods T = 0.2, 1.0, 1.5, 2.0, 2.5, and

TABLE 1. Earthquake Records Used in Statistical Study

Earthquake (1)	Magnitude (2)	Station name (3)	Source distance (km) (4)	Component (5)	Peak acceleration (g) (6)
Northwest California, 10/7/1951	5.8	Ferndale City Hall	56.3	S44W	0.104
				N46W	0.112
San Francisco, 3/22/1957	5.3	San Francisco Golden Gate Park	11.2	N10E	0.083
				S80E	0.105
Helena, Montana, 10/31/1935	6.0	Helena, Montana Carrol College	6.2	S00W	0.146
				S90W	0.145
Parkfield, Calif., 6/27/1966	5.6	Temblor, California #2	59.6	N65W	0.269
				S25W	0.347
San Fernando, 2/9/1971	6.4	Pacoima Dam	7.3	S16E	1.172
				S74W	1.070
		250 E. First Street Basement, Los Angeles	41.4	N36E	0.100
				N54W	0.125
Loma Prieta, 10/17/1989	7.1	Corralitos-Eureka Canyon Road	7.0	90°	0.478
				0°	0.630
		Capitola-Fire Station	9.0	90°	0.398
				0°	0.472
Northridge, 1/17/1994	6.7	Arleta Nordhoff Ave.-Fire Station	9.9	90°	0.344
				360°	0.308
		Pacoima Dam-Down Stream	19.3	265°	0.434
				175°	0.415

TABLE 2. Average Response Ratios for Six-SDOF Structures with Passive Damping

Damping ratio (1)	T = 0.2 s x_{max} (2)	T = 0.2 s a_{max} (3)	T = 1.0 s x_{max} (4)	T = 1.0 s a_{max} (5)	T = 1.5 s x_{max} (6)	T = 1.5 s a_{max} (7)	T = 2.0 s x_{max} (8)	T = 2.0 s a_{max} (9)	T = 2.5 s x_{max} (10)	T = 2.5 s a_{max} (11)	T = 3.0 s x_{max} (12)	T = 3.0 s a_{max} (13)
$\xi_{min} = 0.05$	0.81	0.82	0.81	0.83	0.81	0.84	0.84	0.88	0.86	0.91	0.89	0.95
$\xi_{max} = 0.40$	0.46	0.54	0.42	0.72	0.46	0.94	0.54	1.19	0.56	1.36	0.59	1.55

3.0 s and a structural damping ratio $\beta = 0.05$ are used. Two supplemental passive dampers with damping ratios $\xi = 0.05$ and 0.40 were considered. The structures were subjected to a set of 20 horizontal components of accelerograms listed in Table 1. These records include a range of earthquake magnitudes, epicentral distances, peak ground accelerations, and soil conditions. The relative displacement and absolute acceleration response ratios are computed as the ratio of the peak response of the structure with the supplemental damper-to-the-peak response without the damper. The average response ratios for the 20 records for the six structures are shown in Table 2. Table 2 indicates that for rigid structures (defined in this study as structures with periods <1.5 s) increasing the supplemental damping ratio from 0.05 to 0.40 decreases both the relative displacement and absolute acceleration, whereas for structures with $T \geq 1.5$ s (flexible structures), increasing the supplemental damping ratio decreases the relative displacement but increases the absolute acceleration. Therefore, for flexible structures, reductions in both the displacement and acceleration responses may be possible with a variable damper, i.e., achieving a displacement response close to that obtained with ξ_{max} and an acceleration response close to that obtained with ξ_{min}. For rigid structures, however, the efficiency of using a variable compared to a passive damper is questionable. In the next section, three semiactive control algorithms are discussed and compared with each other to examine the effectiveness of variable dampers in reducing the displacement and acceleration responses of structures.

SEMIACTIVE CONTROL ALGORITHMS

The governing differential equation of motion for an n-degree of freedom structure with mass matrix $\mathbf{M}$, damping matrix $\mathbf{C}$, and stiffness matrix $\mathbf{K}$ with m semiactive dampers subjected to ground acceleration $\ddot{x}_g(t)$ is given by

$$\mathbf{M}\ddot{\mathbf{x}}(t) + \mathbf{C}\dot{\mathbf{x}}(t) + \mathbf{K}\mathbf{x}(t) = \mathbf{D}\mathbf{u}(t) - \mathbf{M}\mathbf{1}\ddot{x}_g(t) \tag{2}$$

where the n-dimensional vector $\mathbf{x}(t)$ represents the relative displacement; the m-dimensional vector $\mathbf{u}(t)$ the control forces generated by the dampers; and the n-dimensional vector $\mathbf{1}$ the unit vector. The matrix $\mathbf{D}$ (size $n \times m$) defines the locations of the control forces generated by the dampers. Using the state-space representation, (2) takes the form

$$\dot{\mathbf{z}}(t) = \mathbf{A}\mathbf{z}(t) + \mathbf{B}\mathbf{u}(t) + \mathbf{H}\ddot{x}_g(t) \tag{3}$$

where $\mathbf{z}(t) = [\mathbf{x}^T(t), \dot{\mathbf{x}}^T(t)]$ is a $2n$-dimensional state vector. The system matrix $\mathbf{A}$ and the matrices $\mathbf{B}$ and $\mathbf{H}$ are given in Soong (1990). Three semiactive control algorithms for regulating the damping coefficient of variable dampers are considered in this study. They include (1) a semiactive LQR; (2) a semiactive generalized LQR; and (3) a semiactive displacement-acceleration domain.

Semiactive LQR Algorithm

This algorithm, referred to herein as SA-1, is the classical LQR that has been extensively used for active control (Soong 1990; Yang et al. 1992) and for semiactive control (Patten et al. 1993, 1994a; Dowdell and Cherry 1994a,b; Symans and Constantinou 1995) of structures. In this algorithm, the control force $\mathbf{u}(t)$ in (2) is selected by minimizing, over the duration of the excitation, the following quadratic expression for the cost function (Soong 1990):

$$J = \int_0^{t_f} [\mathbf{z}^T(t)\mathbf{Q}\mathbf{z}(t) + \mathbf{u}^T(t)\mathbf{R}\mathbf{u}(t)]\,dt \tag{4}$$

where t_f = duration of excitation; and $\mathbf{Q}$ (size $2n \times 2n$) and $\mathbf{R}$ (size $m \times m$) are positive semidefinite and positive definite weighting matrices, respectively. If the elements of $\mathbf{Q}$ are larger than those of $\mathbf{R}$, reducing $\mathbf{z}(t)$ has priority over reducing $\mathbf{u}(t)$. For a closed-loop control configuration, minimizing (4) subject to the constraint of (3) results in a control force vector $\mathbf{u}(t)$ regulated only by the state vector $\mathbf{z}(t)$, such that

$$\mathbf{u}(t) = -\frac{1}{2}\mathbf{R}^{-1}\mathbf{B}^T\mathbf{P}\mathbf{z}(t) = \mathbf{G}\mathbf{z}(t) \tag{5}$$

where matrix $\mathbf{G}$ (size $m \times 2n$) represents the gain matrix; and matrix $\mathbf{P}$ (size $2n \times 2n$) is the solution of the classical Riccati equation, which after neglecting the excitation term reduces to

$$\mathbf{P}\mathbf{A} + \mathbf{A}^T\mathbf{P} - \frac{1}{2}\mathbf{P}\mathbf{B}\mathbf{R}^{-1}\mathbf{B}^T\mathbf{P} + 2\mathbf{Q} = 0 \tag{6}$$

The damping coefficient of damper i at time t can be computed from (5) as

$$c_i^*(t) = \frac{u_i(t)}{\dot{x}_i(t)} = \frac{\sum_{j=1}^{2n} \mathbf{G}_{i,j}\mathbf{z}_j(t)}{\dot{x}_i(t)}, \quad i = 1, m \tag{7}$$

where $\dot{x}_i(t)$ = relative velocity between the ends of damper i. Using the constraints in (1), the damping coefficient is selected as

$$c_i(t) = \begin{cases} c_{min,i} & c_i^*(t) \leq c_{min,i} \\ c_i^*(t) & c_{min,i} < c_i^*(t) < c_{max,i} \\ c_{max,i} & c_i^*(t) \geq c_{max,i} \end{cases} \tag{8}$$

A passive damper with coefficient c_{min} is obtained when $\mathbf{Q}$ in (4) and (6) is a null matrix, and a passive damper with coefficient c_{max} is obtained when the elements of $\mathbf{Q}$ approach infinity.

To examine the effectiveness of this algorithm, two-SDOF structures with periods $T = 0.2$ s and 3.0 s and a structural damping ratio $\beta = 0.05$ are considered. Each structure contains a variable damper with a damping ratio ranging from $\xi_{min} = 0.05$ to $\xi_{max} = 0.40$. The structures are subjected to the 20 ground excitations listed in Table 1. In the analysis, $\mathbf{R}$ is a scalar set equal to $1/\mathbf{K}$ and $\mathbf{Q}$ is selected as [see Wu et al. (1995)]

$$\mathbf{Q} = q\begin{bmatrix} \mathbf{K} & 0 \\ 0 & \mathbf{M} \end{bmatrix} \tag{9}$$

where q = parameter reflecting the importance of the reduction in the state vector $\mathbf{z}(t)$ or the control force vector $\mathbf{u}(t)$. The mean response ratios (the average of the peak displacement or acceleration response with semiactive control divided by their counterparts with no control) for q ranging from 0 to 1.0 are computed and plotted in Fig. 1 for $T = 0.2$ s and in Fig. 2 for

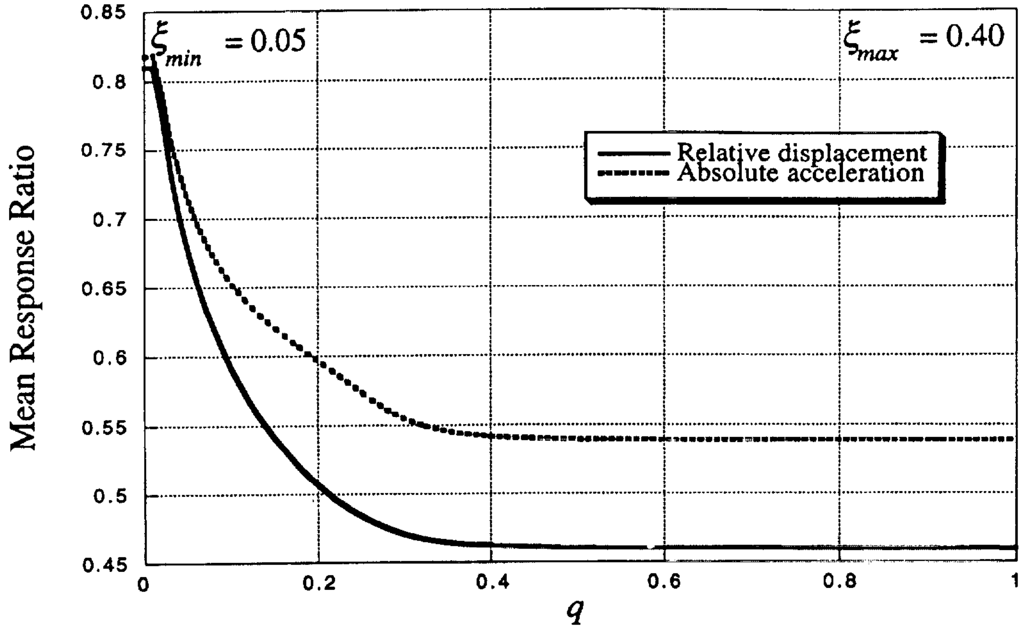

FIG. 1. Variation of Displacement and Acceleration Response Ratios with *q* for SDOF Structure with *T* = 0.2 s Using Algorithm SA-1

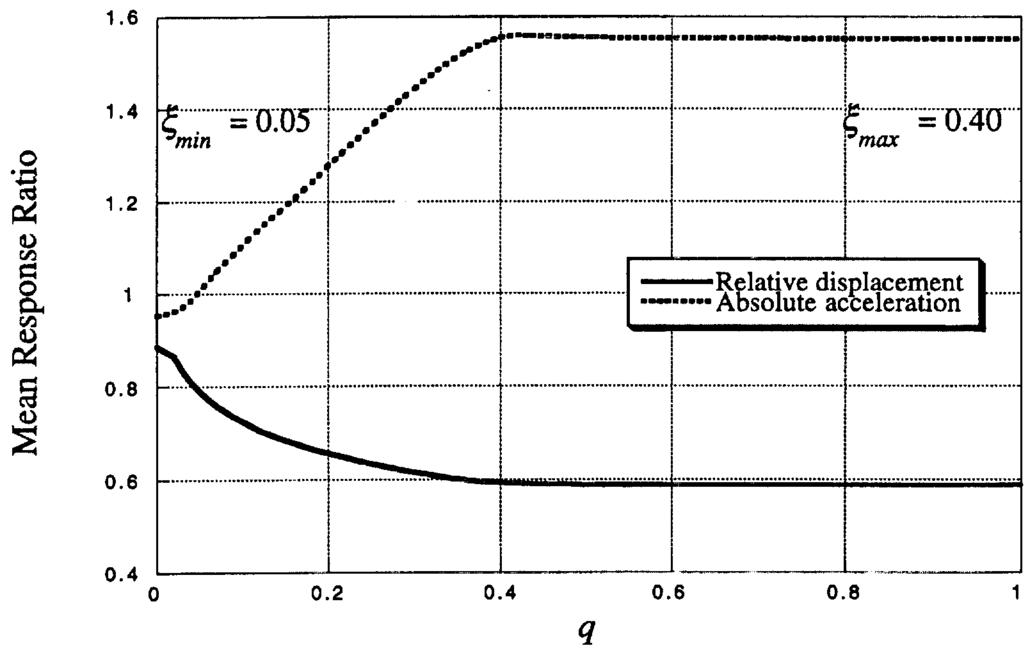

FIG. 2. Variation of Displacement and Acceleration Response Ratios with *q* for SDOF Structure with *T* = 3.0 s Using Algorithm SA-1

$T = 3.0$ s. The plots indicate that for $q = 0$, the mean response ratios are very close to those with a passive damper with $\xi_{min} = 0.05$, and for $q \geq 0.5$, the mean response ratios are nearly the same as those with a passive damper with $\xi_{max} = 0.40$ (compare Columns 2 and 3 of Table 2 with the ordinates at $q = 0$ and 1 in Fig. 1, and Columns 12 and 13 with the ordinates at $q = 0$ and 1 in Fig. 2). For q between 0 and 0.5, the response ratios are between those with passive dampers with ξ_{min} and ξ_{max}. For the structure with $T = 0.2$ s (Fig. 1), increasing q decreases both the relative displacement and absolute acceleration. For the structure with $T = 3.0$ s (Fig. 2), however, increasing q decreases the relative displacement but increases the absolute acceleration. Fig. 1 shows that for the structure with $T = 0.2$ s, a variable damper is inefficient and the use of a passive damper with a damping ratio ξ_{max} is more advantageous.

TABLE 3. Average Response Ratios for Structure (*T* = 3.0 s) with Passive and Semiactive Dampers

Control (1)	Passive, ξ_{min} (2)	Passive, ξ_{max} (3)	SA-1 (4)	SA-2 (5)	SA-3 (6)
x_{max}	0.89	0.59	0.70	0.70	0.70
a_{max}	0.95	1.55	1.15	0.95	1.09

Table 3 (Column 4) shows the average response ratios for the structure with $T = 3.0$ s, where q is adjusted to give a displacement response ratio of 0.70 ($q = 0.12$). This ratio is selected as a baseline for comparing the responses from the three algorithms. Table 3 indicates that, compared with a passive damper with ξ_{max} (Column 3), using the SA-1 algorithm increases the relative displacement by 0.11 (11%) (the x_{max} and

a_{max} in Table 3 are percentages of the uncontrolled response) and reduces the absolute accelerations by 0.40 (40%).

Semiactive Generalized LQR Algorithm

This algorithm, referred to herein as SA-2, was introduced by Yang et al. (1992) for active control of structures and is adopted for semiactive control in this study. In this algorithm, the cost function is augmented by imposing a penalty on the absolute acceleration of each degree of freedom to control the acceleration response of the structure. The generalized cost function has the form

$$J = \int_0^{t_f} [\mathbf{z}^T(t)\mathbf{Q}\mathbf{z}(t) + \ddot{\mathbf{x}}_a^T(t)\mathbf{Q}_a\ddot{\mathbf{x}}_a(t) + \mathbf{u}^T(t)\mathbf{R}\mathbf{u}(t)]\,dt \quad (10)$$

in which $\ddot{\mathbf{x}}_a(t)$ = absolute acceleration vector; and $\mathbf{Q}_a$ (size $n \times n$) = symmetric positive semidefinite weighting matrix. If the elements of $\mathbf{Q}_a$ are larger than those of $\mathbf{Q}$, reducing the absolute acceleration vector $\ddot{\mathbf{x}}_a(t)$ has priority over reducing the state vector $\mathbf{z}(t)$. The absolute acceleration vector $\ddot{\mathbf{x}}_a(t)$ is computed from (2) as

$$\ddot{\mathbf{x}}_a(t) = \mathbf{A}_0\mathbf{z}(t) + \mathbf{B}_0\mathbf{u}(t) \quad (11)$$

where $\mathbf{A}_0 = [-\mathbf{M}^{-1}\mathbf{K}, -\mathbf{M}^{-1}\mathbf{C}]$ and $\mathbf{B}_0 = \mathbf{M}^{-1}\mathbf{D}$. Thus, the cost function takes the form

$$J = \int_0^{t_f} [\mathbf{z}^T(t), \mathbf{u}^T(t)] \begin{bmatrix} \mathbf{Q} + \mathbf{A}_0^T\mathbf{Q}_a\mathbf{A}_0 & \mathbf{A}_0^T\mathbf{Q}_a\mathbf{B}_0 \\ \mathbf{B}_0^T\mathbf{Q}_a\mathbf{A}_0 & \mathbf{R} + \mathbf{B}_0^T\mathbf{Q}_a\mathbf{B}_0 \end{bmatrix} \begin{bmatrix} \mathbf{z}(t) \\ \mathbf{u}(t) \end{bmatrix} dt \quad (12)$$

Minimizing (12) subject to the constraint of (3) results in a control force vector $\mathbf{u}(t)$ given by

$$\mathbf{u}(t) = -\frac{1}{2}\tilde{\mathbf{R}}^{-1}(\mathbf{B}^T\tilde{\mathbf{P}} + 2\mathbf{B}_0^T\mathbf{Q}_a\mathbf{A}_0)\mathbf{z}(t) = \tilde{\mathbf{G}}\mathbf{z}(t) \quad (13)$$

where $\tilde{\mathbf{G}}$ (size $m \times 2n$) = gain matrix; and $\tilde{\mathbf{P}}$ (size $2n \times 2n$) is the solution to the classical Riccati equation which takes the form

$$\tilde{\mathbf{P}}\tilde{\mathbf{A}} + \tilde{\mathbf{A}}^T\tilde{\mathbf{P}} - \frac{1}{2}\tilde{\mathbf{P}}\mathbf{B}\tilde{\mathbf{R}}^{-1}\mathbf{B}^T\tilde{\mathbf{P}} + 2\tilde{\mathbf{Q}} = 0 \quad (14)$$

in which

$$\tilde{\mathbf{R}} = \mathbf{R} + \mathbf{B}_0^T\mathbf{Q}_a\mathbf{B}_0; \quad \tilde{\mathbf{A}} = \mathbf{A} - \mathbf{B}\tilde{\mathbf{R}}^{-1}\mathbf{B}_0^T\mathbf{Q}_a\mathbf{A}_0 \quad (15a,b)$$

$$\tilde{\mathbf{Q}} = \mathbf{Q} + \mathbf{A}_0^T\mathbf{Q}_a\mathbf{A}_0 - \mathbf{A}_0^T\mathbf{Q}_a\mathbf{B}_0\tilde{\mathbf{R}}^{-1}\mathbf{B}_0^T\mathbf{Q}_a\mathbf{A}_0 \quad (15c)$$

Similar to the SA-1 algorithm, the damping coefficient of damper i at time t can be expressed as

$$c_i^*(t) = \frac{u_i(t)}{\dot{x}_i(t)} = \frac{\sum_{j=1}^{2n} \tilde{G}_{i,j}z_j(t)}{\dot{x}_i(t)}, \quad i = 1, m \quad (16)$$

where $\dot{x}_i(t)$ = relative velocity between the ends of damper i. Imposing the constraints in (1), the damping coefficient will be

$$c_i(t) = \begin{cases} c_{\min,i} & c_i^*(t) \le c_{\min,i} \\ c_i^*(t) & c_{\min,i} < c_i^*(t) < c_{\max,i} \\ c_{\max,i} & c_i^*(t) \ge c_{\max,i} \end{cases} \quad (17)$$

For a null $\mathbf{Q}_a$ matrix, the SA-2 algorithm reduces to the SA-1 algorithm.

The two SDOF structures with T = 0.2 and 3.0 s with a variable damper were analyzed using the SA-2 algorithm. The same scalar $\mathbf{R} = 1/\mathbf{K}$ and matrix $\mathbf{Q}$ [(9)] with $q = 0.5$ for both T = 0.2 s and T = 3.0 s are used in this example. It should be noted that $q = 0.5$ results in a response approximately the same as that using a passive damper with $\xi_{max} = 0.40$ (see Figs. 1 and 2). For SDOF systems, $\mathbf{Q}_a$ is a scalar and equal to q_a which reflects the importance of the reduction in the state vector $\mathbf{z}(t)$ or in the acceleration response vector $\ddot{\mathbf{x}}_a(t)$.

The mean displacement and acceleration response ratios for the two-SDOF structures subjected to the 20 accelerograms for q_a ranging from 10^0 to 15^5 for T = 0.2 s and 10^3 to 10^7 for T = 3.0 s are shown in Figs. 3 and 4, respectively. The figures indicate that for small q_a the response with a variable damper is close to that with a passive damper with $\xi_{max} = 0.40$ (compare Columns 2 and 3 of Table 2 with Fig. 3, and Columns 12 and 13 with Fig. 4). Fig. 3 indicates that for the structure with T = 0.2 s, increasing q_a increases both the displacement and acceleration responses, and again the variable damper is not as efficient as a passive damper with a damping ratio $\xi_{max} = 0.40$. Fig. 4 indicates that for the structure with T = 3.0 s, the variable damper is effective in significantly reducing the acceleration response while slightly increasing the displacement response.

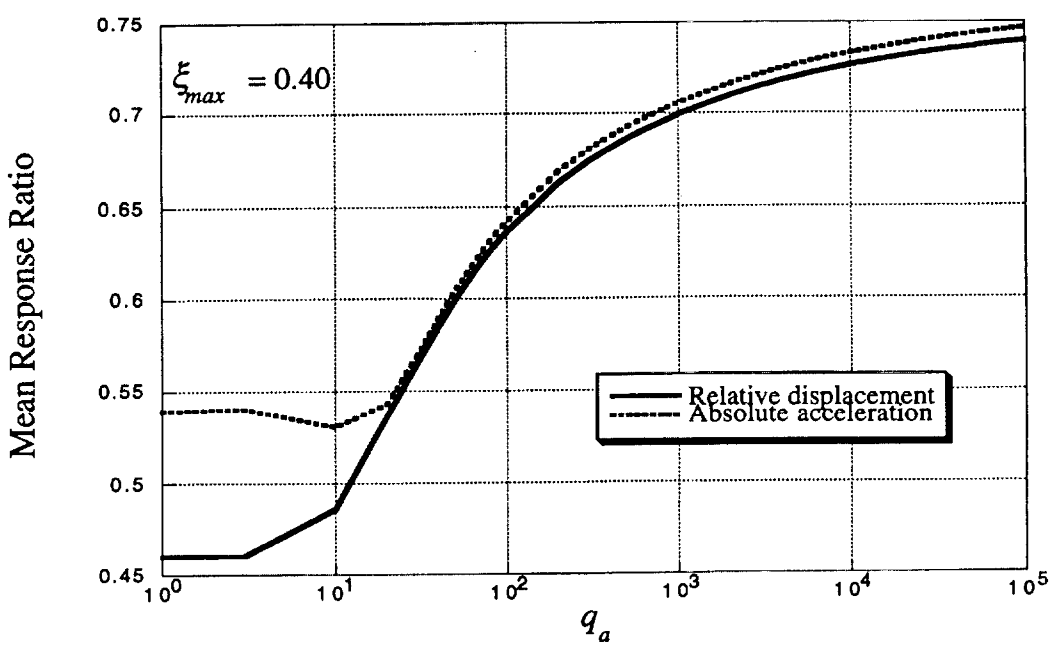

FIG. 3. Variation of Displacement and Acceleration Response Ratios with q_a for SDOF Structure with T = 0.2 s Using Algorithm SA-2

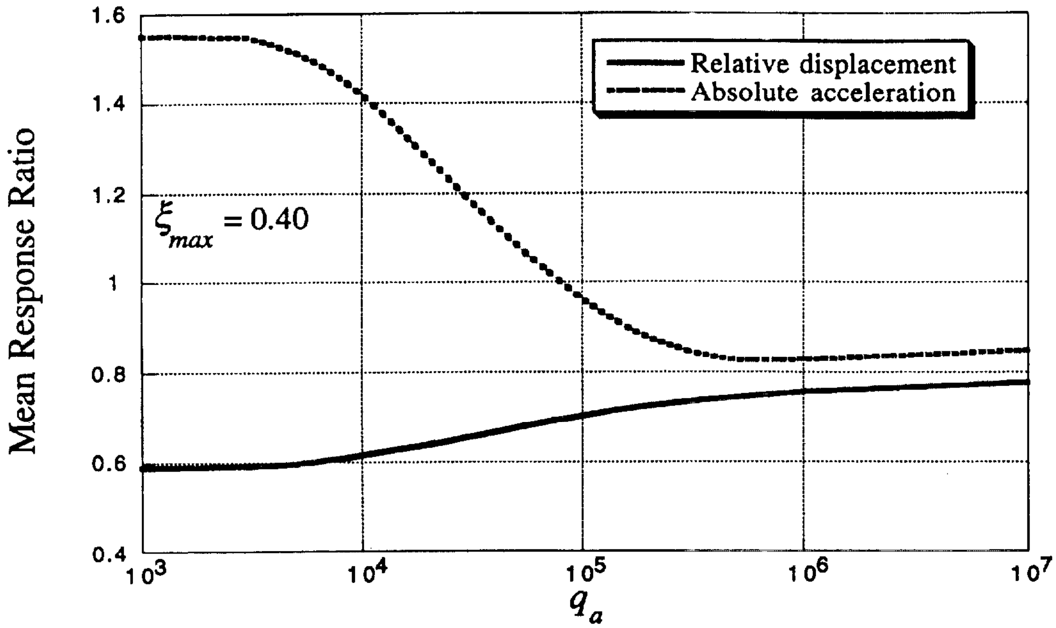

FIG. 4. Variation of Displacement and Acceleration Response Ratios with q_a for SDOF Structure with $T = 3.0$ s Using Algorithm SA-2

Shown in Table 3 (Column 5) are the mean response ratios for the structure with $T = 3.0$ s, where q_a is adjusted to give a mean displacement response ratio of 0.70 ($q_a = 1.0 \times 10^5$). Table 3 shows that compared with a passive damper with $\xi_{max} = 0.40$ (Column 3), the SA-2 algorithm increases the relative displacement by 11%, but it decreases the absolute accelerations by 60% [the acceleration response is the same as that with a passive damper with $\xi_{min} = 0.05$ (see Column 2 of Table 3)]. This demonstrates the effectiveness of the SA-2 algorithm in reducing the acceleration response.

Semiactive Displacement-Acceleration Domain Algorithm

This algorithm, referred to herein as SA-3, is a refinement of the bang-bang algorithm presented by Feng and Shinozuka (1990, 1993). The refinement assumes a displacement-acceleration domain (Fig. 5), where the horizontal axis represents the relative displacement response and the vertical axis the absolute acceleration response normalized to a reference parameter Ω. This parameter, which has the unit of s^{-2}, is used as a weighting factor to impose different penalties on the displacement and acceleration responses. At any time t, the response may be represented by a single point on the displacement-acceleration domain. The angle $\theta(t)$ between the horizontal axis and the line connecting the origin to the response point (Fig. 5) is used to select the damping coefficient. This angle is expressed as

$$\theta(t) = \tan^{-1} \frac{|\ddot{x}_a(t)|/\Omega}{|x(t)|} \tag{18}$$

A small $\theta(t)$ indicates a large displacement response with respect to the normalized acceleration and consequently requiring a higher damping coefficient. The opposite is true for a large $\theta(t)$. It is therefore desirable to assign a large damping coefficient c_{max} for small θ ($0 \le \theta(t) \le \theta_1$) and a small damping coefficient c_{min} for large θ ($\pi/2 - \theta_1 \le \theta(t) \le \pi/2$), where the angle θ_1 is yet to be determined. A linear variation of the damping coefficient with $\theta(t)$ is used for $\theta_1 \le \theta(t) \le \pi/2 - \theta_1$ (see Fig. 5). The damping coefficient may be selected as follows:

$$c(t) = \begin{cases} c_{min} & \pi/2 - \theta_1 \le \theta(t) \le \pi/2 \\ c_{max} - \dfrac{c_{max} - c_{min}}{\dfrac{\pi}{2} - 2\theta_1}[\theta(t) - \theta_1] & \theta_1 < \theta(t) < \pi/2 - \theta_1 \\ c_{max} & 0 \le \theta(t) \le \theta_1 \end{cases} \tag{19}$$

Eq. (18) indicates that increasing Ω decreases $\theta(t)$, which results in selecting a large $c(t)$. Consequently, reducing the relative displacement has priority over reducing the absolute acceleration. The opposite is true for decreasing Ω. The reference parameter Ω, therefore, reflects the importance of reductions in displacements or accelerations.

Contrary to the first two algorithms (SA-1 and SA-2), which depend on the structural properties (stiffness, damping, and mass), the SA-3 algorithm depends on the measured response only [(18) and (19)]. The SA-3 algorithm is, therefore, robust with respect to the uncertainties in estimating the structural parameters.

The two-SDOF structures with $T = 0.2$ and 3.0 s with var-

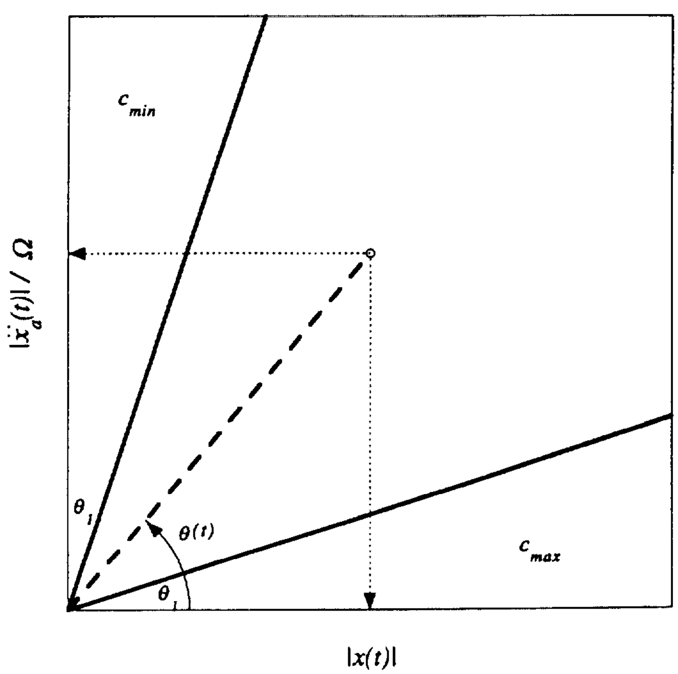

FIG. 5. Displacement-Acceleration Domain for Algorithm SA-3

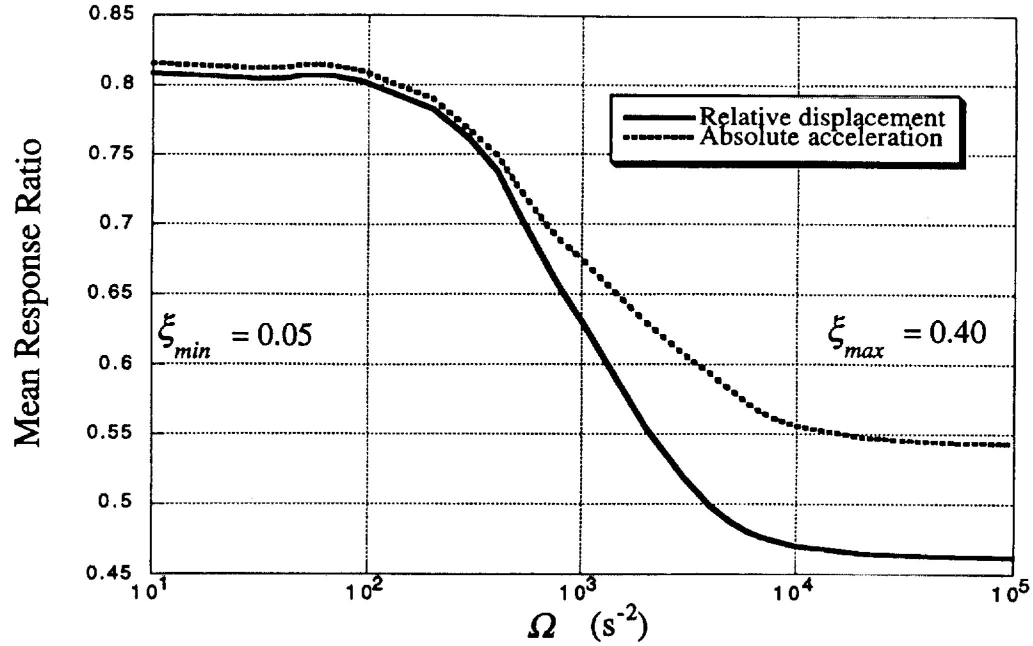

FIG. 6. Variation of Displacement and Acceleration Response Ratios with Ω for SDOF Structure with $T = 0.2$ s Using Algorithm SA-3

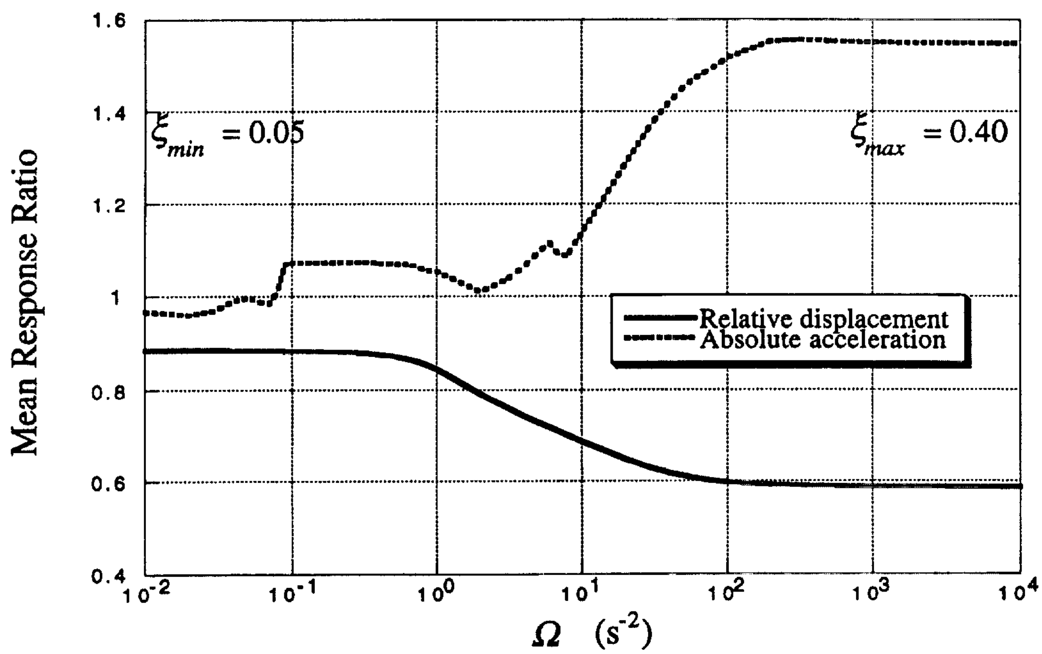

FIG. 7. Variation of Displacement and Acceleration Response Ratios with Ω for SDOF Structure with $T = 3.0$ s Using Algorithm SA-3

iable dampers are analyzed using the SA-3 algorithm. Different values for θ_1 were assumed. It was found that a θ_1 between $\pi/10$ and $\pi/30$ resulted in the largest reductions in the response. The mean displacement and acceleration response ratios for the 20 records for $\theta_1 = \pi/10$ and for Ω ranging from 10^1 to 10^5 s^{-2} for $T = 0.2$ s and 10^{-2} to 10^4 s^{-2} for $T = 3.0$ s are plotted in Figs. 6 and 7, respectively. Figs. 6 and 7 indicate that for a small Ω the response is approximately the same as that with a passive damper with $\xi_{min} = 0.05$, and for a large Ω the response is nearly the same as that with a passive damper with $\xi_{max} = 0.40$ (compare Columns 2 and 3 of Table 2 with Fig. 6, and Columns 12 and 13 with Fig. 7). Fig. 6 shows that for the structure with $T = 0.2$ s, a semiactive control is inefficient and that a passive damper with ξ_{max} is more advantageous.

Table 3 (Column 6) shows the mean response ratios for the structure with $T = 3.0$ s, where the value of Ω is adjusted to give a mean displacement response ratio of 0.70 ($\Omega = 8$ s^{-2}). Table 3 indicates that compared with a passive damper with ξ_{max}, the SA-3 algorithm increases the relative displacement by 11% and reduces the absolute accelerations by 46%.

Analysis and Comparisons of Algorithms

Based on the analyses and the results presented, the following may be concluded:

1. Variable dampers are more effective than passive dampers in reducing the seismic response of flexible structures (defined in this study as structures with $T \geq 1.5$ s), where increased damping has opposite effects on the displacement and acceleration responses. Examples of these structures include base-isolated structures, tall buildings, and isolated and cable-stayed bridges. For rigid struc-

tures (defined in this study as structures with $T < 1.5$ s), however, variable dampers are not effective in improving the response as compared to passive dampers.

2. Based on the results in Table 3, the generalized LQR algorithm (SA-2) is more effective in reducing the response than the other two algorithms. The use of the SA-2 algorithm results in an acceleration response nearly the same as that with a passive damper with a low damping ratio ($\xi_{min} = 0.05$), while the displacement response is increased by only 11% compared with a passive damper with a high damping ratio ($\xi_{max} = 0.40$). The effectiveness of the SA-2 algorithm results from the penalty imposed on controlling the absolute acceleration response.
3. Both the SA-1 and the SA-3 algorithms result in similar responses (Table 3). The SA-3 algorithm, however, is somewhat preferable to SA-1, since it is inherently robust with respect to structural uncertainties.

APPLICATIONS

Two examples are presented to demonstrate the performance of variable dampers in reducing the seismic response of structures. The first is a bridge modeled as an SDOF, and the second is a six-story base-isolated frame modeled as an MDOF.

Bridge

A bridge modeled as an SDOF structure was used to assess the effectiveness of the algorithms in reducing the seismic response. The bridge is similar to that used by Feng and Shinozuka (1990, 1993). It has a mass of 1.02×10^6 kg, a hybrid control system consisting of an isolator with a stiffness 3,300 kN/m, and a variable damper. The damping ratio for the bridge is assumed as 2%, and the damping coefficient of the variable damper varies between $c_{min} = 150$ kN·s/m and $c_{max} = 1,200$ kN·s/m. The bridge was subjected to four accelerograms—the N21E component of Taft Lincoln School Tunnel, Wheeler Ridge Earthquake, 1954; the S74W component of Pacoima Dam, San Fernando Earthquake, 1971; the 0° component of the Corralitos Eureka Canyon Road, the Loma Prieta Earthquake, 1989; and the 90° component of the Arleta Nordhoff Avenue Fire Station, the Northridge Earthquake, 1994—each scaled to a peak ground acceleration of 1.0g. The results of the analyses with no control and with passive control (passive damper) with damping coefficients c_{min} and c_{max} are shown in Table 4 (Columns 2–7) that indicate that an increase in damping decreases the relative displacements and increases the absolute accelerations.

The bridge with a variable damper was analyzed using the three algorithms. For the SA-1 algorithm, the scalar $\mathbf{R}$ is set equal to $1/\mathbf{K}$ and the matrix $\mathbf{Q}$ is computed by (9). By varying q, different combinations of displacements and accelerations are obtained. Table 4 (Columns 8 and 9) shows the responses for a $q = 0.12$, where it is observed that x_{max} and a_{max} are between those obtained with c_{min} and c_{max}. For the SA-2 algorithm, the analysis was carried out with a $q = 0.6$ and different values of q_a. The results for a $q_a = 3 \times 10^5$ are shown in Table 4 (Columns 10 and 11), where it is noted that the displacement responses are close to (or even lower than) those with c_{max} and the acceleration responses are close to those with c_{min}. For the SA-3 algorithm, the analysis was carried out for $\theta_1 = \pi/10$ and different Ω values. The results presented in Table 4 (Columns 12 and 13) are for an $\Omega = 7$ s^{-2}. Similar to the SA-1 algorithm, the responses are between those with a low and a high damping coefficient. The results in Table 4 underscore the advantage of using the SA-2 algorithm.

Base-Isolated Frame

A six-story base-isolated frame was considered to examine the effectiveness of the three algorithms in reducing the displacement and acceleration responses of an MDOF structure. The column stiffnesses are $k_i = 3 \times 10^5$ kN/m, floor masses $m_i = 1.0 \times 10^5$ kg, and the damping ratio is assumed to be 5% in each mode. The frame is supported at its base by an isolator with a linear stiffness $k_b = 9,000$ kN/m, a mass $m_b = 1.4 \times 10^5$ kg, and a variable damper with damping coefficients between $c_{min} = 100$ kN·s/m and $c_{max} = 900$ kN·s/m. Tables 5 and 6 show the responses with passive dampers to the S74W component of Pacoima Dam, San Fernando Earthquake, 1971; and the N21E component of Taft Lincoln School Tunnel, Wheeler Ridge Earthquake, 1954; both scaled to a peak ground acceleration of 1.0g. Tables 5 and 6 indicate (Columns 2–7 in each table) that an increase in the damping coefficient of the isolator decreases the displacements and increases the absolute accelerations.

The frame was also analyzed with a variable damper at the base using the three algorithms. For the SA-1 algorithm, the

TABLE 4. Response of Bridge with No Control and with Passive and Semiactive Dampers

Control (1)	No Control x_{max} (m) (2)	No Control a_{max} (g) (3)	Passive, c_{min} x_{max} (m) (4)	Passive, c_{min} a_{max} (g) (5)	Passive, c_{max} x_{max} (m) (6)	Passive, c_{max} a_{max} (g) (7)	SA-1 x_{max} (m) (8)	SA-1 a_{max} (g) (9)	SA-2 x_{max} (m) (10)	SA-2 a_{max} (g) (11)	SA-3 x_{max} (m) (12)	SA-3 a_{max} (g) (13)
Taft, 1954	0.250	0.083	0.236	0.085	0.181	0.137	0.199	0.122	0.175	0.079	0.197	0.125
Pacoima Dam, 1971	0.170	0.056	0.144	0.050	0.114	0.086	0.118	0.074	0.106	0.048	0.116	0.074
Corralitos, 1989	0.297	0.098	0.246	0.083	0.157	0.137	0.183	0.107	0.151	0.088	0.182	0.091
Arleta, 1994	0.488	0.161	0.411	0.143	0.308	0.218	0.140	0.195	0.350	0.128	0.358	0.185

TABLE 5. Response of Six-Story Base-Isolated Frame to Pacoima Dam Accelerogram

Level (1)	Passive, c_{min} x_{max} (m) (2)	Passive, c_{min} a_{max} (g) (3)	Passive, c_{max} x_{max} (m) (4)	Passive, c_{max} a_{max} (g) (5)	SA-1 x_{max} (m) (6)	SA-1 a_{max} (g) (7)	SA-2a x_{max} (m) (8)	SA-2a a_{max} (g) (9)	SA-2b x_{max} (m) (10)	SA-2b a_{max} (g) (11)
Top	0.150	0.256	0.115	0.302	0.136	0.282	0.115	0.266	0.116	0.242
5	0.150	0.245	0.115	0.279	0.136	0.263	0.115	0.246	0.116	0.230
4	0.149	0.226	0.114	0.258	0.135	0.238	0.114	0.227	0.115	0.226
3	0.147	0.203	0.114	0.213	0.134	0.213	0.113	0.198	0.114	0.204
2	0.145	0.208	0.112	0.223	0.132	0.212	0.112	0.211	0.112	0.200
1	0.143	0.212	0.111	0.245	0.130	0.224	0.110	0.224	0.110	0.210
Base	0.139	0.212	0.108	0.261	0.127	0.239	0.107	0.235	0.108	0.223

TABLE 6. Response of Six-Story Base-Isolated Frame to Taft Accelerogram

Level (1)	Passive, c_{min} x_{max} (m) (2)	Passive, c_{min} a_{max} (g) (3)	Passive, c_{max} x_{max} (m) (4)	Passive, c_{max} a_{max} (g) (5)	SA-1 x_{max} (m) (6)	SA-1 a_{max} (g) (7)	SA-2a x_{max} (m) (8)	SA-2a a_{max} (g) (9)	SA-2b x_{max} (m) (10)	SA-2b a_{max} (g) (11)
Top	0.170	0.337	0.141	0.428	0.161	0.370	0.134	0.378	0.136	0.396
5	0.169	0.311	0.140	0.392	0.160	0.340	0.133	0.370	0.135	0.374
4	0.167	0.273	0.138	0.322	0.158	0.286	0.132	0.324	0.134	0.336
3	0.164	0.278	0.135	0.326	0.155	0.305	0.129	0.319	0.132	0.333
2	0.161	0.308	0.132	0.392	0.151	0.357	0.127	0.345	0.129	0.346
1	0.157	0.334	0.128	0.432	0.147	0.384	0.124	0.362	0.127	0.343
Base	0.153	0.351	0.124	0.447	0.143	0.404	0.121	0.360	0.124	0.330

R matrix is a scalar and is set equal to 1, and the **Q** matrix is computed from (9). Similar to the SDOF case, different displacement and acceleration responses are obtained by varying q. Columns 6 and 7 of Tables 5 and 6 show the responses when $q = 700$, where the absolute accelerations are reduced and the displacements are increased when compared with the response with a passive damper with c_{max}.

For the analysis using the SA-2 algorithm, **R** is set equal to 1, and the matrix **Q** is computed from (9) using $q = 5{,}000$ that results in a response approximately equal to that with a passive damper with c_{max}. The $\mathbf{Q}_a$ matrix is selected as

$$\mathbf{Q}_a = \mathbf{q}_a\mathbf{I} \tag{20}$$

where **I** = identity matrix (size 7 × 7). By varying q_a different penalties can be imposed on the state and acceleration vectors. It was found that with $q_a = 1.5 \times 10^5$, a displacement close to that obtained with a passive damper with damping coefficient c_{max} and an absolute acceleration close to that obtained with damping coefficient c_{min} were obtained as shown in Tables 5 and 6 (Columns 8 and 9). To further reduce the acceleration response of the isolator, a higher penalty was imposed on its absolute acceleration by changing the element that corresponds to the isolator acceleration in the identity matrix—Element (7,7)—to a larger number (7 instead of 1) and using a $q_a = 10^5$. This change resulted in a further reduction in the acceleration response of the frame as shown in Tables 5 and 6 (Columns 10 and 11).

A similar analysis was performed to investigate the effectiveness of SA-3 algorithm for the base-isolated MDOF structure, where the displacement-acceleration domain was defined using the isolator response. The analysis (results are not included) showed that the algorithm was not effective, and the accelerations obtained were greater than those using a passive damper with damping coefficient c_{max}.

CONCLUSIONS

The overall objective of this study was to investigate the effectiveness of variable dampers in reducing the response of structures to earthquake loading. Three semiactive control algorithms are presented and compared. They include: (1) an LQR algorithm referred to as SA-1 that has been used extensively in active and semiactive control of structures; (2) a generalized LQR algorithm referred to as SA-2 with a penalty imposed on the acceleration response that was introduced by Yang et al. (1992) for active control and adopted in this study for semiactive control; and (3) a displacement-acceleration domain algorithm referred to as SA-3, where the damping coefficient is selected based on the location of the response parameters on the displacement-acceleration plane.

Two-SDOF structures (a flexible and a rigid) were analyzed with the three algorithms using 20 accelerograms for the excitation. The results indicate the following:

1. Variable dampers can be effective in reducing the acceleration response and consequently seismic forces in flexible structures, such as base-isolated and tall buildings and isolated and cable-stayed bridges, where an increase in damping adversely affects the acceleration response. Variable dampers, however, are not effective for rigid structures as compared to passive dampers.
2. The SA-2 algorithm is more efficient than the other two in reducing the displacement and acceleration responses. The efficiency of this algorithm is mostly due to the penalty imposed in controlling the absolute acceleration response.
4. The SA-1 and SA-3 algorithms result in similar efficiency in reducing the response of SDOF structures, although the SA-3 algorithm is more robust.

The three algorithms were used to compute the seismic response of an isolated bridge modeled as an SDOF structure and a base-isolated frame modeled as an MDOF structure. The results indicate that for these two structures, which can be classified as flexible, variable dampers are quite effective in reducing the displacement and acceleration responses. The SA-3 algorithm, however, is not effective for MDOF structures.

ACKNOWLEDGMENTS

This study was supported by the Structures Division, Building and Fire Research Laboratory, National Institute of Standards and Technology, U.S. Department of Commerce, Gaithersburg, Maryland through a grant to the Mechanical Engineering Department, Southern Methodist University, Dallas, Texas.

APPENDIX I. REFERENCES

Calise, A. J., and Sweriduk, G. D. (1994). "Active damping of building structures using robust control." *Proc., U.S. 5th Nat. Conf. Earthquake Engrg.*, Earthquake Engrg. Research Inst., El Cerrito, Calif., 1023–1032.

Dowdell, D. J., and Cherry, S. (1994a). "Structural control using semiactive friction dampers." *Proc., 1st World Conf. on Struct. Control*, Int. Assoc. for Structural Control, Los Angeles, Calif., FA1/59–FA1/68.

Dowdell, D. J., and Cherry, S. (1994b). "Semi-active friction dampers for seismic response control of structures." *Proc., U.S. 5th Nat. Conf. Earthquake Engrg.*, Earthquake Engrg. Research Inst., El Cerrito, Calif., 819–828.

Feng, Q., and Shinozuka, M. (1990). "Use of a variable damper for hybrid control of bridge response under earthquake." *Proc., U.S. Nat. Workshop on Struct. Control*, Univ. of Southern California, Los Angeles, Calif., 107–112.

Feng, Q., and Shinozuka, M. (1993). "Control of seismic response of bridge structures using variable dampers." *J. Intelligent Mat. Sys. and Struct.*, 4, 117–122.

Kawashima, K., and Unjoh, S. (1993). "Variable dampers and variable stiffness for seismic control of bridges." *Proc., Int. Workshop on Struct. Control*, U.S. Panel on Structural Control Research, Los Angles, Calif., 283–297.

Kawashima, K., Unjoh, S., and Mukai, H. (1994). "Seismic response control of highway bridges by variable damper." *Proc., U.S. 5th Nat. Conf. Earthquake Engrg.*, Earthquake Engrg. Research Inst., El Cerrito, Calif., 829–838.

Loh, C. H., and Ma, M. J. (1994). "Active-damping or active-stiffness control for seismic excited buildings." *Proc., 1st World Conf. on Struct. Control*, Int. Assoc. for Structural Control, Los Angeles, Calif., TA2/11–TA2/20.

Patten, W. N., He, Q., Kuo, C. C., Liu, L., and Sack, R. L. (1994b). "Suppression of vehicle induced bridge vibration via hydraulic semi-active vibration dampers (SAVD)." *Proc., 1st World Conf. on Struct. Control*, Int. Assoc. for Structural Control, Los Angeles, Calif., FA1/30–FA1/38.

Patten, W. N., Kuo, C. C., He, Q., Liu, L., and Sack, R. L. (1994a). "Seismic structural control via hydraulic semi-active vibration dampers (SAVD)." *Proc., 1st World Conf. on Struct. Control*, Int. Assoc. for Structural Control, Los Angeles, Calif., FA2/83–FA2/89.

Patten, W. N., Sack, R. L., and He, Q. (1996). "Controlled semi-active hydraulic vibration absorber for bridges." *J. Struct. Engrg.*, ASCE, 122(2), 187–192.

Patten, W. N., Sack, R. L., Yen, W., Mo, C., and Wu, H. C. (1993). "Seismic motion control using semi-active hydraulic force actuators." *Proc., ATC-17-1 Seminar on Seismic Isolation, Passive Energy Dissipation, and Active Control*, Vol. 2, Appl. Technol. Council, Redwood City, Calif., 727–736.

Sack, R. L., Kuo, C. C., Wu, H. C., Liu, L., and Patten, W. N. (1994). "Seismic motion control via semi-active hydraulic actuators." *Proc., U.S. 5th Nat. Conf. Earthquake Engrg.*, Earthquake Engrg. Research Inst., El Cerrito, Calif., 311–320.

Sadek, F., Mohraz, B., Taylor, A. W., and Chung, R. M. (1996). "Passive energy dissipation devices for seismic applications." *Rep. No. NISTIR 5923*, Nat. Inst. of Standards and Technol., Gaithersburg, Md.

Soong, T. T. (1990). *Active structural control: Theory and practice.* John Wiley & Sons, Inc., Nnew York, N.Y.

Symans, M. D., and Constantinou, M. C. (1995). "Development and experimental study of semi-active fluid damping devices for seismic protection of structures." *Rep. No. NCEER-95-0011*, State Univ. of New York at Buffalo, Buffalo, N.Y.

Wu, Z., Soong, T. T., Gattuli, V., and Lin, R. C. (1995). "Nonlinear control algorithms for peak response reduction." *Tech. Rep. No. NCEER-95-0004*, Nat. Ctr. for Earthquake Engrg. Res., Buffalo, N.Y.

Yang, C., and Lu, L. W. (1994). "Seismic response control of cable-stayed bridges by semi-active friction damping." *Proc., U.S. 5th Nat. Conf. Earthquake Engrg.*, Earthquake Engrg. Research Inst., El Cerrito, Calif., 911–920.

Yang, J. N., Akbarpour, A., and Ghaemmaghami, P. (1987). "New optimal control algorithms for structural control." *J. Engrg. Mech.*, ASCE, 113(9), 1369–1386.

Yang, J. N., Li, Z., and Vongchavalitkul, S. (1992). "A generalization of optimal control theory: Linear and nonlinear structures." *Rep. No. NCEER-92-0026*, State Univ. of New York at Buffalo, Buffalo, N.Y.

Yang, J. N., Li, Z., Wu, J. C., and Kawashima, K. (1994). "Aseismic hybrid control of bridge structures." *Proc., U.S. 5th Nat. Conf. Earthquake Engrg.*, Earthquake Engrg. Research Inst., El Cerrito, Calif., 861–870.

APPENDIX II. NOTATION

The following symbols are used in this paper:

$\mathbf{A}$ = system matrix;
a_{max} = maximum absolute acceleration response;
$\mathbf{B}$ = control force location matrix in state-space;
$\mathbf{C}$ = damping matrix;
$c(t)$ = damping coefficient of variable damper;
c_{max} = maximum damping coefficient;
c_{min} = minimum damping coefficient;
$\mathbf{D}$ = control force location matrix;
$\mathbf{G}$ = gain matrix;
g = gravity acceleration;
$\mathbf{H}$ = excitation location matrix in state-space;
$\mathbf{I}$ = identity matrix;
J = performance index;
$\mathbf{K}$ = stiffness matrix;
k_b = isolator stiffness;
$\mathbf{M}$ = mass matrix;
m = number of dampers;
m_b = isolator mass;
n = number of degrees of freedom;
$\mathbf{P}$ = Riccati matrix;
$\mathbf{Q}$ = weighting matrix;
$\mathbf{Q}_a$ = weighting matrix;
q = parameter or multiplier;
q_a = parameter or multiplier;
$\mathbf{R}$ = weighting matrix;
T = natural period;
t = time;
t_f = duration of excitation;
$\mathbf{u}$ = control force vector;
$\mathbf{x}$ = displacement vector;
$\ddot{\mathbf{x}}_a$ = absolute acceleration response vector;
$\ddot{x}_g$ = ground acceleration;
x_{max} = maximum relative displacement;
$\mathbf{z}$ = state vector;
$\theta(t)$ = angle defining response in displacement-acceleration domain;
ξ_{max} = maximum damping coefficient of variable dampers;
ξ_{min} = minimum damping coefficient of variable dampers; and
Ω = reference parameter.